2015

Functional Characterization of a Drosophila Transgenic Line Expressing a Chimeric Flightin: Implications on Flight Muscle Structure and Mating Behavior

Harshal Athalye
University of Vermont

Functional Characterization of a *Drosophila* Transgenic Line Expressing a Chimeric Flightin: Implications on Flight Muscle Structure and Mating Behavior

An Honors College Senior Thesis Defense Presented

by

Harshal Athalye

to

Dr. Jim O Vigoreaux

Dr. Judith Van Houten

Dr. Laura Hill

of

The University of Vermont

April 30, 2015

I. Abstract:

The asynchronous, indirect flight muscles (IFM) of *Drosophila* are characterized by their remarkable crystalline myofilament lattice structure that has been proposed to have evolved to power skilled flight for survival, and to produce male courtship song, a sexually selected pre-mating behavior for reproduction. It is not known how physiologically and genetically IFM generates two distinct behaviors under separate evolutionary schemes. Flightin, a 20kDa myofibrillar myosin-binding protein that in *Drosophila* is exclusively expressed in the IFM, is required for muscle structural integrity and flight. The flightin N-terminal sequence (~65 aa in *D. melanogaster*) is highly variable among *Drosophila* species, unlike the rest of the *Drosophila* protein. Using electron microscopy, fourier image analyses, flight and wing beat frequency tests, I explored the hypothesis that the sequence of amino acids in flightin's N-terminal region has a strong influence on myofilament lattice spacing and crystallinity. This is investigated by the creation of two independent *D.melanogaster* transgenic fly lines expressing a *D.virilis-D.melanogaster* chimeric flightin, both of which exhibit larger myofillament lattice spacing compared to the full length transgenic and *D.virilis* control fly lines, along with an intermediate wing beat frequency and an equal and/or improved flight ability compared to the control full length transgenic line. These results suggest the N-terminal region is under evolutionary pressures to optimize crystalline lattice structure.

II. Background:

i. Insect Flight Muscle

From a morphological and physiological standpoint, insect flight muscle is categorized as synchronous, whereby the rate of contraction matches the rate of motor neuron firing or as asynchronous, which is present only in insects and utilizes mostly myogenic activity and contract independent of neural stimulation.

Insect flight muscles are further functionally categorized into direct flight muscles (DFM) and indirect flight muscles (IFM). The DFM lie ventral to the wings and are directly attached to the base of the wings, contraction of which produces ventral movement of the wings. The IFM, which are composed of dorsal longitudinal and dorsal ventral muscles, induce wing movement by changing the position of the tergum, the dorsal plate of the thorax, as shown below. (Dudley 2000, Snodgrass 1935)

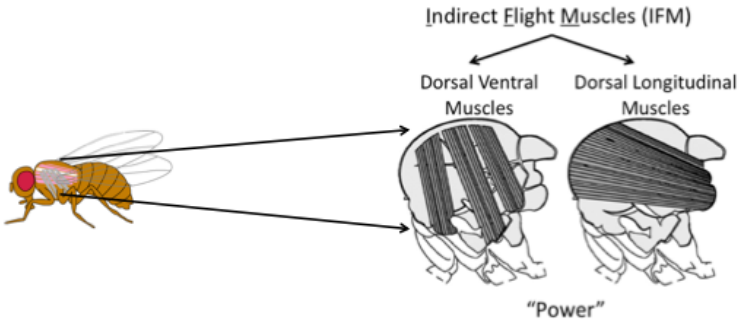

Figure 1: Dorsal ventral and dorsal longitudinal muscles of IFM. (Dickinson 2005)

Drosophila fibrillar muscles are of major importance in this study as they include the major power generating IFM; oriented 12 fibers oriented longitudinally, and 14 ventrally which are densely packed with mitochondria in order to provide the high demand of metabolic energy to power flight, and generate vibrations to produce the male courtship song, an important pre-copulatory behavior as shown in Figure 2.

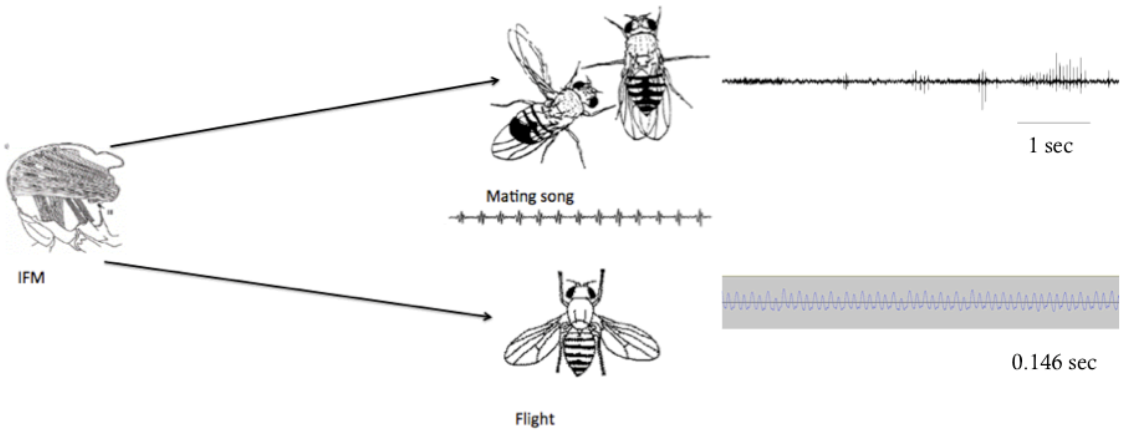

Figure 2: The important functions of the *Drosophila* IFM. The IFM generates the power for flight and the rhythmic wing vibrations of the mating song. Male courtship song, and wing beat frequency oscillograms are shown on the right.

Another possible evolutionary advantage that can be attributed to enhancing flight power is the highly regular and ordered lattice arrangement of thick and thin filaments as revealed by electron microscopy. The architecture of a myofibril cross-sectional area shows a double hexagonal array of one thick filament surrounded by six thin filaments, with a thin to think filament ratio of 3:1. Although the specifics of how this geometric lattice regularity is attained and could drive skilled flight is not clear, some possibilities include the notion that a regular lattice geometry enables force to be transmitted more efficiently along the length of the myofibrils, and hence muscle fibers leading to a more efficient power output (Chakravorty 2013*)*. The lattice structure could also influence the coordinated cross-bridge binding and rate or amplitude of force development (Iwamoto *et al* 2006*)*.

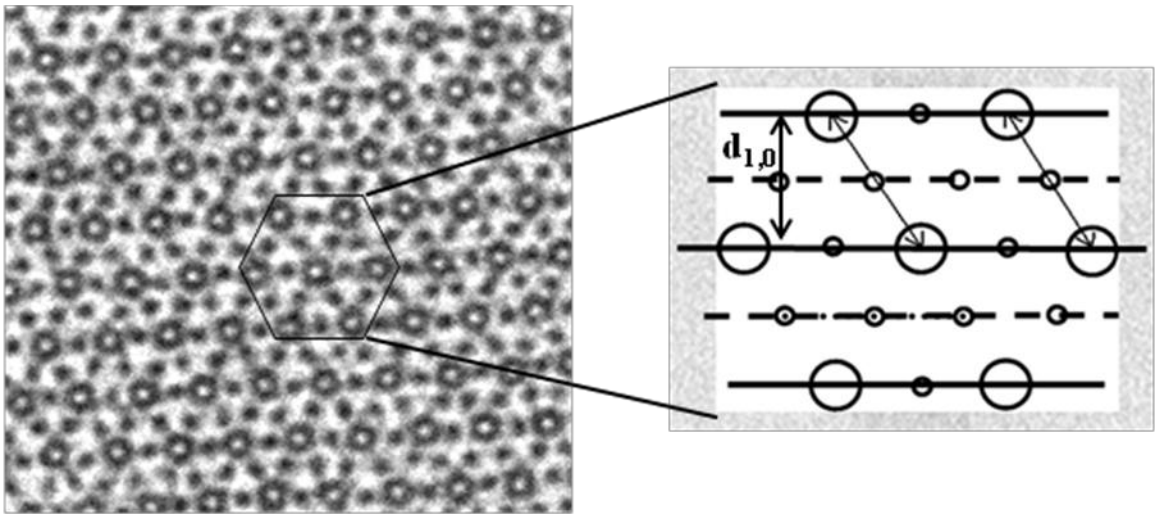

Figure 3: Cross-section electron micrograph of *Drosophila* indirect flight muscle myofibrils showing the double hexagonal array of hollow thick and filled thin filaments. The right panel shows a cartoon of the lattice arrangement where the bigger circles represent thick filaments and the smaller circles represent thin filaments. The $d_{1,0}$ lattice spacing is the distance between the consecutive thick filament planes (vertical two-headed arrow), from where the center to center spacing between thick filaments, or inter-thick filament spacing (angled two-headed arrows) could be retrieved. Figure used with permission from (Chakravorty 2013).

ii. Role of flightin in flight muscle structure and function

Flightin is a 20-kDa myofibrillar protein that in *Drosophila melanogaster* is expressed exclusively in IFM (Vigoreaux *et al* 1993). Previous studies suggest that flightin plays an essential role in normal sarcomere structure, contractile activity, and that it interacts with the thick filament backbone. Flightin is required for normal thick filament assembly and maintains muscle and thick filament structural integrity in active muscle through its interaction with the myosin rod (Reedy *et al* 2000, Ayer *et al* 2003). Flightin sequence analysis across 12 *Drosophila* species revealed that flightin consists of 3 putative domains that differ in sequence conservation: N-terminal domain, (65 aa, ~ 20% conserved); C-terminal domain, (44 aa, ~ 59% conserved); and a middle "WYR" domain, (58 aa, ~ 92% conserved). Previous studies have examined transgenic flies expressing flightin with truncated N-terminal and C-terminal domains to examine the effects on muscle structure and function.

Drosophila with a null mutation in the flightin gene (fln^0), are viable but flightless and unable to produce the male courtship song due to age- dependent degeneration of their flight musculature (Reedy *et al* 2000). Flightin null IFM thick filaments and sarcomeres from late stage pupa are, on average, about 30% longer than in wild-type IFM, suggesting that flightin plays a major role in thick filament assembly during myofibrillogenesis. The fln^0 thick filaments are about 30-40% more compliant than wild type thick filaments (Contompasis *et al* 2010). These structural and functional abnormalities in fln^0 are fully rescued with the introduction of a full-length normal flightin transgene, fln^+(Barton *et al* 2005). The results show that flightin is an important protein for *Drosophila* IFM development, structure and function (Contompasis *et al* 2010). It is not clear how flightin's contribution to thick filament stiffness is related to its role in thick filament assembly process *in vivo*. It is also still not clear how flightin stiffens the thick filament or maintains normal sarcomeric regularity. Flightin sequence analysis shows high conservation ~59% in the C-terminal region among *Drosophila* species, suggesting that its function may be taxon-specific. The truncation of the 44 amino acids from the flightin C-terminal ($fln^{\Delta C44}$) abolished flight and the ability to generate the male courtship song, even with some partial rescue in IFM structural and mechanical properties, compared to that in complete absence of flightin, fln^0 (Tanner *et al* 2011). IFM fibers generated significantly reduced oscillatory work and power output with reduced underlying cross-bridge kinetics compared to the rescued control null fibers (fln^+), suggesting that the partial rescue in $fln^{\Delta C44}$ sarcomere structure was not sufficient for myofibrillar stability and normal contractile kinetics. The marked reduction in cross-

bridge kinetics could be due to the sarcomeric structural aberrations like abnormalities in M/Z lines, or A-band breaks (Tanner *et al* 2011).

Recent research done by Samya Chakravorty (Chakravorty 2013), investigated an N-terminal truncated flightin transgenic line ($fln^{\Delta N62}$) and it's effect on muscle structure and function. The deletion of the N-terminal domain did not show a dominant negative effect, as the N-terminal deleted allele expressed in a fln^{+} background behaved similarly to the control fln^{+} line. The $fln^{\Delta N62}$ line was capable of flight and production of an abnormal male courtship song, although a decrease in flight ability accompanied by a decrease in fiber power output compared to fln^{+}. Electron microscopy showed that the myofilament lattice structural organization and order are reduced compared to that of the fln^{+} control line, suggesting that a highly ordered myofilament lattice is essential for normal power output. In addition, mating competition assays showed that wild-type females consistently selected fln^{+}males over $fln^{\Delta N62}$ males, suggesting that the flightin N-terminal domain contributes to mating song attributes that may be under sexual selection (Chakravorty, 2013).

This study extrapolates on the previous work of the N-terminal truncated flightin transgenic line ($fln^{\Delta N62}$) done by Samya Chakravorty. The purpose of this study is to establish the influence of amino acid sequences in flightin N-terminal domain on myofilament lattice structure through the use of transgenic *D.melanogaster* lines that express a chimeric flightin consisting of a *D.virilis* N-terminal domain and a *D.melanogaster* WYR and C-terminal domains. My hypothesis is that the charge on the amino acids in the N-terminal domain of flightin influence the myofilament lattice

spacing due to electrostatic repulsion or attraction between the negatively charged thick filaments and the flightin N-terminal region.

The Vigoreaux lab selected the N-terminal region of *D. virilis* specifically due to the fact that it contains low amino acid sequence similarity with the N-terminal region of *D. melanogaster* and also because *D.virilis* and *D. melanogaster* courtship songs differ in important song parameters of the sine song and pulse song. The sine song is used to stimulate female flies, and the pulse song contains the interpulse interval, a parameter used for species recognition.

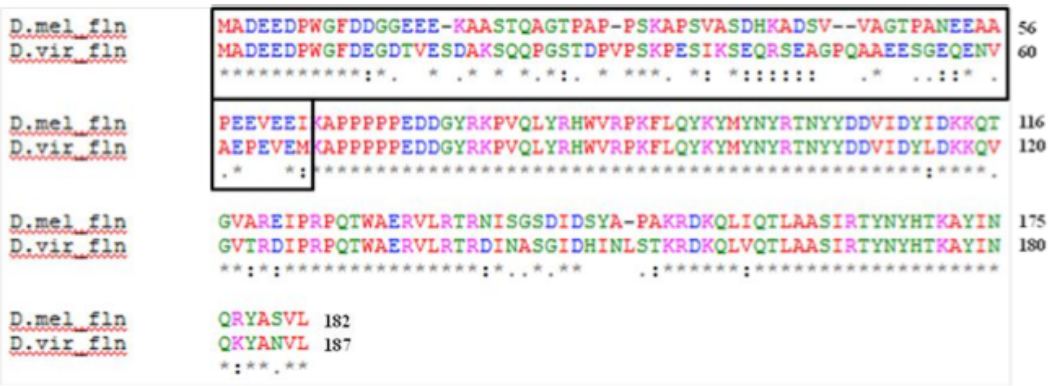

Figure 4: Sequence alignment of flightin amino acids from *D.melanogaster* and *D.virilis* with the variable N-terminal domain boxed in. Identities are marked by asterisks (*). Colon (:) indicates residues at that position are very similar based on their properties, and dot (.) indicates residues at that position are more or less similar. Figure used with permission from (Chakravorty 2013)

The boxed portion Figure 4 above represents the N-terminal region (67 aa) of both *D.melanogaster,* and *D.virilis.* The letters represent specific amino acid letter codes. Red letters are indicative of non-polar amino acids, blue represents acidic amino acids, green represents polar amino acids, and pink represents basic amino acids.

For this study, four distinct lines were tested, 3 *D. melanogaster* lines, and 1 *D. virilis* line: (i) two independent homozygous chimeric transgenic strains on a fln^{0} background and will hence be referred to as $fln^{virnch95}$ and $fln^{virnch96}$; (ii) The first control

contains an endogenous flightin, which is null, and a transgenic full length flightin, and will hence be referred to as *fln*$^{+}$; (iii) The second control is a *D.virilis* wildtype. Two independent chimeric lines were created to make sure phenotypes and other experimental results seen are not due to position effects (i.e., insertion of the transgene interfering with expression of other genes). Using the following four lines, I performed flight tests, wing beat frequency tests, and fourier image analyses on myofibril EM cross-sections to help support the idea that the sequence of amino acids in the N-terminal region influence aspects of myofilament lattice structure. In addition, mating competition assays were initiated to determine if expression of the chimeric flightin influences mate selection by *D. melanogaster* and *D. virilis* females.

III. Methods:

Fly Rearing All flies were raised at 22°C and 70% humidity with 12:12 light:dark cycles in an environmental room and fed standard corn meal food. Flies were contained in one of two ways: a 25 x 95 mm polypropylene fly vials (Fisher Scientific), and 6 oz. square bottom polypropylene bottles (Genesse Scientific). Flies were transferred and collected with the use of CO_2, however, excessive use of CO_2 was avoided. Males and females were aged 3-5 days after eclosion, and separated into individual vials for 24 hours before wing-beat frequency and flight tests were conducted.

Wing-beat frequency The wing-beat frequency (WBF) tests were carried out in the INSECTAVOX, a custom made apparatus equipped with a particle velocity sensitive microphone that gives a high signal to noise ratio. Precautions were taken to reduce excess noise interference by placing the device away from the windows to minimize vibrations. Proper aged 2 day old flies were collected using CO_2, fishing line was

krazzy™ glued to the head of the fly in-betweens the eyes making sure the glue did not come in contact with the eyes, or the thorax. The fly was allowed to recover from the CO_2 in a food vial for 24 hours. After the 24 hours forceps were used to hold the fly with the use of the fishing line. The use of the Audacity program on Mac is necessary to obtain the WBF. Once the INSECTAVOX is turned on, hit record on the Audacity program making sure the auxiliary cord on the Mac is set as "input", and that the project rate is at 44,100 Hz. The fly was held over the microphone making sure the fly was beating its wings for a minimum of 10 seconds. The fly was then moved away from the microphone, making sure to leave a 5 second interval of complete silence before holding the fly over the microphone again for a minimum of 10 seconds. This process was repeated until the fly was held over the microphone for a total of 6 times for a minimum of 10 seconds for each individual fly. A fast fourier transform of the sound bite was analyzed in a logarithmic graph to obtain the WBF. The averages of the 6 trials will provide the wing beat frequency value of each individual fly. Once 25 males and 25 females per line have been assigned an individual wing beat frequency value an ANOVA T-test statistical analysis was conducted whereby the chimeric line will be compared against each of the controls to determine whether the wing beat frequency values are statistically significant by calculating a p-value. For each individual line, the mean, the standard error of the mean and variance will be calculated in order to compare individual flies within their specific lines and represented by generating bar graphs.

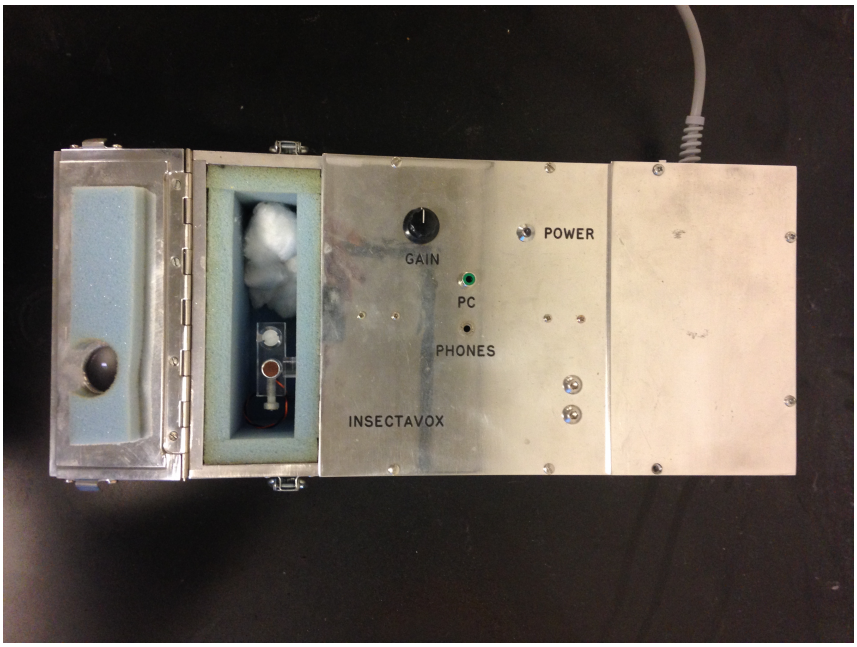

Figure 5: INSECTAVOX apparatus, left side panel opened to reveal a particle velocity sensitive microphone.

Flight tests The flight tests were conducted in a flight box with a light shinning from the top. The flies were released through an opening on the side and their flight trajectory was tracked based on the quadrants they landed in, quadrant 0 being the bottom of the box (no flight), and 6 being the top. Each fly was tested 6 times. Once 25 males and 25 females have been assigned an individual average flight score, an ANOVA T-test statistical analysis was conducted whereby the chimeric lines were individually compared against each of the controls to determine whether the mean flight scores are statistically significant by calculating a p-value. For each individual line, the mean, the standard error of the mean and variance was calculated in order to compare individual flies within their specific lines and represented by generating bar graphs.

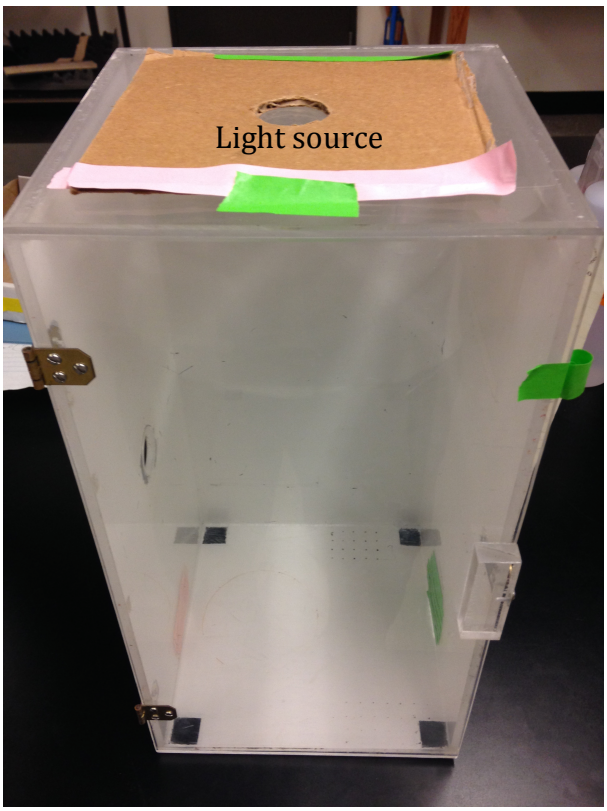

Figure 6: Flight test apparatus used, light source is placed on top. Flies enter through circular hole on left wall.

Transmission Electron Microscopy

i. Sample Preparation The thorax was isolated from the rest of the fly, and bisected carefully using the forceps pick tool in Karnovsky's solution. Once bisected the section is fixed overnight in 4^{o}C in Karnovsky's fixative (2.5% glutaraldehyde, 1.0% paraformaldehyde in 0.1M Cacodylate buffer, pH 7.2). The tissue was again rinsed in Cacodylate buffer, followed by dehydration through graded ethanols, cleared in propylene oxide and embedded in Spurr's epoxy resin. Semi-thin sections (1 μm) were cut with glass knives on a Reichert ultracut microtome, stained with methylene blue – azure II, and evaluated for areas of interest. Ultrathin sections (60-80 nm) were cut with a diamond knife, retrieved onto 200 mesh thin bar nickel grids, contrasted with uranyl

acetate (2% in 50% ethanol) and lead citrate, and examined with a JEOL 1400 TEM (JEOL USA, Inc, Peabody, Ma) operating at 60kV.

ii. Image analysis Images of the sectioned thoraces were collected at 8000X magnification and 1.48807nm pixel size.

iii. Fast Fourier Transform of myofibrils Fast Fourier Transform of the myofibrils were created and measured using the program ImageJ and the procedure outlined in (Chakravorty 2013). All cross section images with same magnification were selected without contrast enhancement, brightness modification and/or changing image size. Full cross-section of a single myofibril was selected and copied to a new image with 512×512 or 1024×1024 pixel size to make sure only myofilaments are included in the image as shown below in the snapshot.

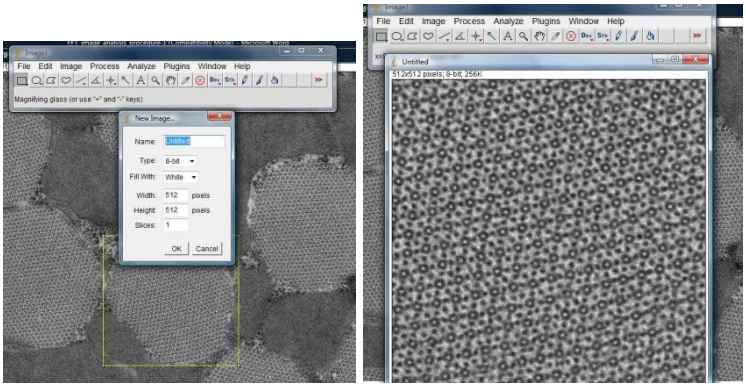

ImageJ FFT tab was selected to obtain the following image as shown below.

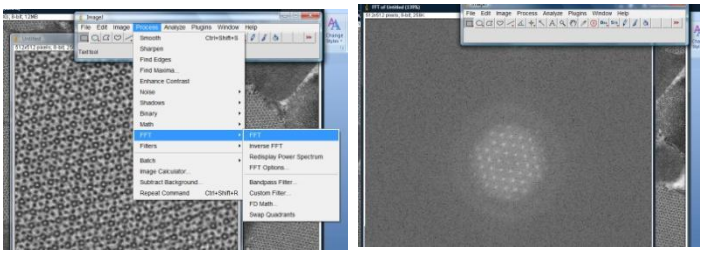

In order to quantify inter-filament distance, pixel size (eg.: 14.26Å) in the original EM

image was noted down. FFT image was scaled, by drawing a horizontal line as shown below to obtain the length in pixel size.

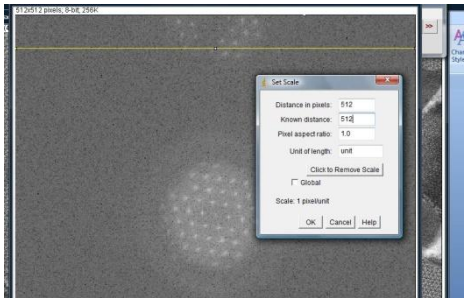

The distance from the center to the 1st order reflection in the FFT was measured by drawing a line, making sure it passed through the center. The length was measured by selecting the tab *analyze-measure* and was divided by the number of inter-spot distances included in the line. In this example, the length of the line is 114.242 pixels and the number of spots passing through the line is seven, and thus the empty spaces between the spots is six. The distance excluding the dots was measured by dividing 114.242 by 6 (number of empty spaces between)

Total number of pixels of FFT × distance / pixel (from the original image) should be constant. Therefore, 512 × 14.26 Å = 19.04 × inter-filament distance ($d_{1,0}$).

Example: $d_{1,0}$ = 512 × 14.26 Å / 19.04 = 383.46 Å or 38.35 nm. Therefore, inter-thick filament distance = $2/\sqrt{3} \times d_{1,0}$ = 38.35 × $2/\sqrt{3}$ = 44.28 nm.

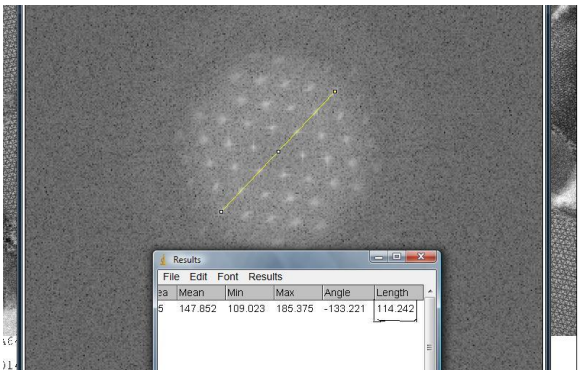

Order or regularity of the lattice as a measure of resolution of the fourier power spectrum and the sharpness of the 1,0 FFT spot intensities:

Resolution was measured by drawing a line connecting as many spots as can be seen across both sides of the center as shown in the image below. The distance in pixels of the line was measured and divided by 2 (eg. 138.593/2 spots= 69.3 pixel resolution in Fourier space). Resolution of the myofilament lattice was calculated as the total number of pixels of FFT × distance per pixel (from the original image) divided by pixel resolution in fourier space. In this example, 512 × 1.426 nm / 69.3 = 10.54 nm resolution.

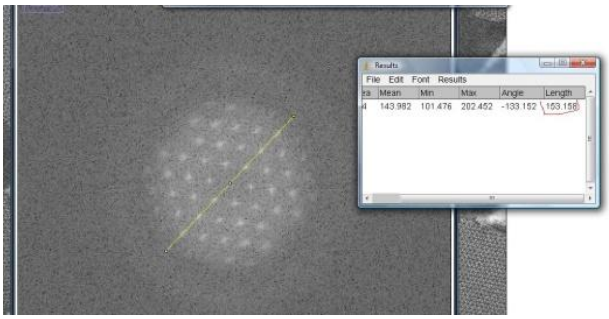

Sharpness was measured from FFT images which were transformed from Cartesian coordinates to polar coordinates using *polar transform plugin* tab in ImageJ.

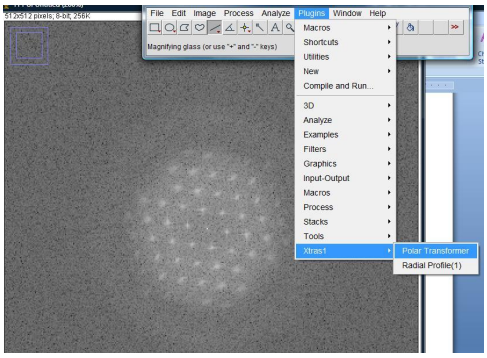

A line along the (1,0) spots were drawn and intensity profile was plotted.

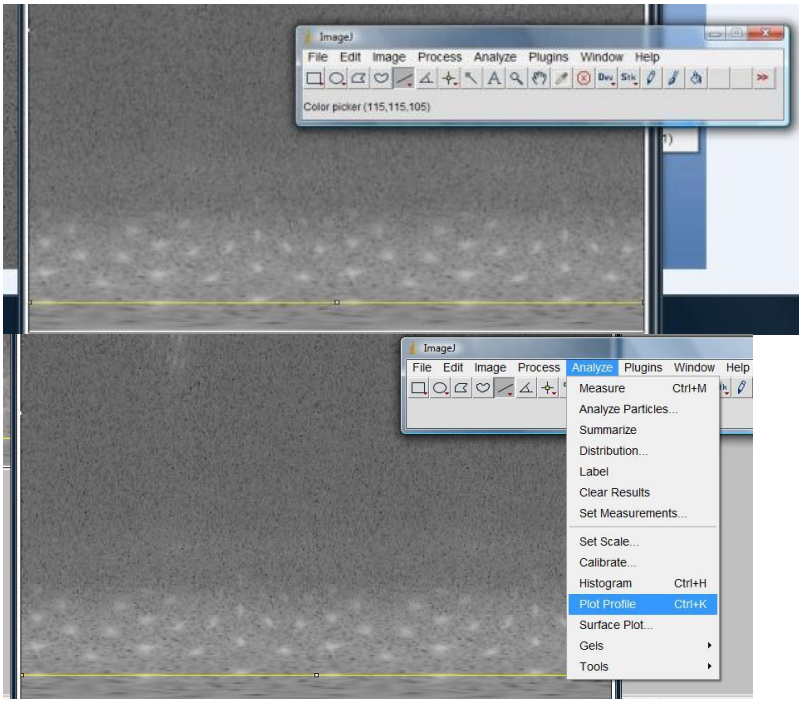

From the intensity *profile plot*, the log of peak height of the spot intensities and the width at half maximum of the intensity peaks were measured from a baseline as shown below for each of the 6 spots in the 1,0 reflection plane and then averaged.

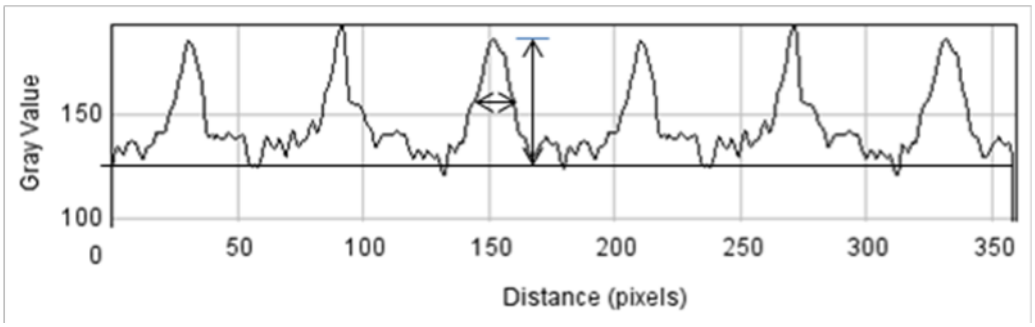

The log of peak height and the width at the half maximum of the intensities are a measure

of the spot sharpness and provide an estimate of the regularity of the lattice. Lower peak intensities and broader half width will indicate more variability in the spacing between lattice planes across the cross section of the myofibril.

Mating Competition Assays Virgin females and males were collected using CO_2; however subsequent use of CO_2 was avoided. After collecting the virgin males and females, they were placed in separate individual vials and aged 3 days after eclosion, as this was the typical age they reached sexual maturity. *D.virilis* females reached sexual maturity at 5 days after eclosion. On the day of testing, the males and females were aspirated into custom-made cylindrical chambers that contained one small opening. The temperature and humidity was recorded and a camcorder mounted on a tripod was used to obtain video documentation of the courtship ritual.

The following competition assays were performed:

	Competition Assay # 1	Competition Assay # 2	Competition Assay # 3	Competition Assay # 4
Male 1	fln^{+}	*D. virilis*	fln^{+}	*D. virilis*
Male 2	$fln^{virnch95}$ or $fln^{virnch96}$	$fln^{virnch95}$ or $fln^{virnch96}$	$fln^{virnch95}$ or $fln^{virnch96}$	$fln^{virnch95}$ or $fln^{virnch96}$
Female	*D.melanogaster*	*D.virilis*	*D.virilis*	*D.melanogaster*

From the videos, successful copulation was scored first, the most definitive endpoint for the assay. In the absence of such courtship index (CI), the fraction of the total recording time the male displayed courtship behaviors (orienting, chasing, tapping, licking, singing, copulation attempts) and wing extension index (WEI), the fraction of the total recording time the male extends and vibrates a wing was recorded. An average value

for the CI and WEI was assigned for each male fly, the standard deviation within group, and the standard error of the mean were calculated. An One-way ANOVA average courtship comparison between the chimeric and control lines was performed, and a bar graph with error bars of standard error of mean was generated to note the least significant differences.

IV. Results:

The flight ability of each fly line was analyzed through two major tests: flight tests and wing beat frequency tests. Transgenic flies (combined males and females) expressing chimeric flightin showed either no difference in flight ability compared to a transgenic control *D. melanogaster* flightin (3.6 ± 0.10 $fln^{virnch96}$ vs. 3.6 ± 0.11 fln^{+} control; p = 0.707; Figure 7), or improved flight ability (4.2 ± 0.09 $fln^{virnch95}$ vs. 3.6 ± 0.11 fln^{+} control, p < 0.005). *D.virilis* showed better flight ability compared to a transgenic control expressing *D. melanogaster* (4.2 ± 0.09 *D.virilis* vs. 3.6 ± 0.11 fln^{+} control; p < 0.005). Male *D.virilis* showed a difference compared to only fln^{+} (4.4 ± 0.15 *D.virilis* vs. 3.3 ± 0.13 fln^{+} control; p = 0.04), all other males in each line were not significantly different from each other. *D.virilis* females showed significantly better flight ability compared to fln^{+} (3.9 ± 0.2 *D.virilis* vs. 3.3 ± 0.15 fln^{+} control; p = 0.009) and $fln^{virnch96}$ (3.9 ± 0.2 *D.virilis* vs. 3.1 ± 0.21 $fln^{virnch96}$; p < 0.005). Female $fln^{virnch95}$ showed significantly better flight ability compared to fln^{+} (3.9 ± 0.2 $fln^{virnch95}$ vs. 3.3 ± 0.15 fln^{+} ; p < 0.005). Female $fln^{virnch96}$ showed poor flight ability compared to $fln^{virnch95}$ (3.1 ± 0.4 $fln^{virnch96}$ vs. 4.0 ± 0.16 $fln^{virnch95}$; p < 0.005).

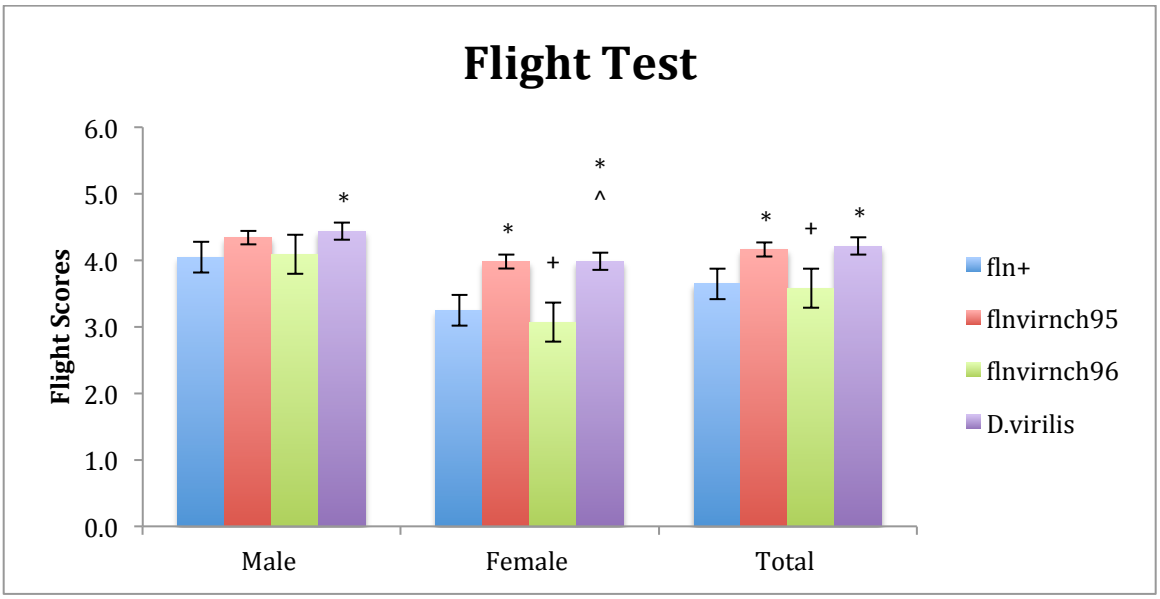

Figure 7: Each bar represents mean ± SEM. Asterisks (*) indicate significant difference ($p < 0.05$) compared to control fln^{+}. Plus signs (+) indicate significant difference ($p < 0.05$) compared to $fln^{virnch95}$. Carrot signs (^) indicate significant difference ($p < 0.05$) compared to $fln^{virnch96}$.

The second test, wing beat frequency (WBF) for the chimeric lines (combined males and females): $fln^{virnch95}$ (185 ± 3 Hz), and $fln^{virnch96}$ (185 ± 3 Hz) was intermediate between that of *D. melanogaster* (202 ± 2 Hz) and *D. virilis* (169 ± 1 Hz), but significantly different from both ($p < 0.005$ $fln^{virnch95}$ vs. fln^{+} control ; $p < 0.005$ $fln^{virnch95}$ vs. *D.virilis*) and ($p < 0.005$ $fln^{virnch96}$ vs. fln^{+} control ; $p < 0.005$ $fln^{virnch96}$ vs. *D.virilis*). The same pattern of $fln^{virnch95}$ and $fln^{virnch96}$ WBF being intermediate between fln^{+} control and *D.virilis* control was observed in males and females separately as seen in Figure 8.

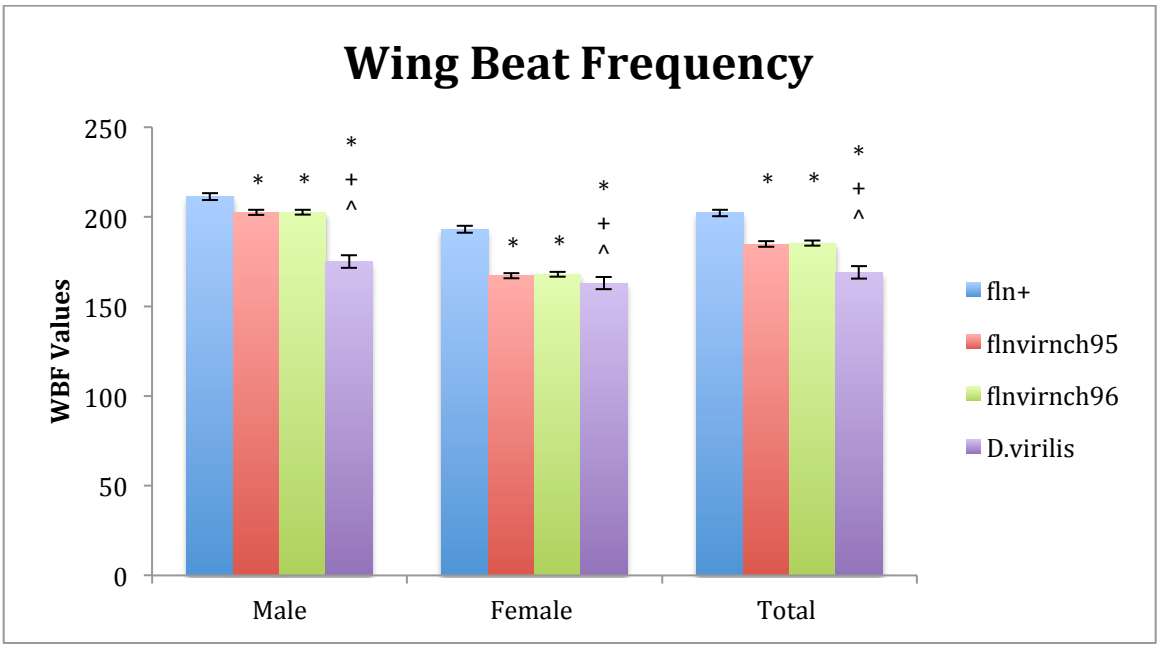

Figure 8: Each bar represents mean ± SEM. Asterisks (*) indicate significant difference ($p < 0.05$) compared to control fln^{+}. Plus signs (+) indicate significant difference ($p < 0.05$) compared to $fln^{virnch95}$. Carrot signs (^) indicate significant difference ($p < 0.05$) compared to $fln^{virnch96}$.

Both the flight tests and WBF graphs consistently show that the male mean is higher than the female mean for all 4 lines.

The significant differences $p<0.05$ for both the flight test scores and WBF prompted the search to see if the differences in the flight ability for the different fly lines can be attributed to differences in myofilament lattice structure of the flight muscle. Electron microscopy cross-sections of both fln^{virnch} lines look similar compared to the control fln^{+} with respect to double hexagonal myofilament arrays, and linear alignment as shown in Figures 9,10,11, and 12.

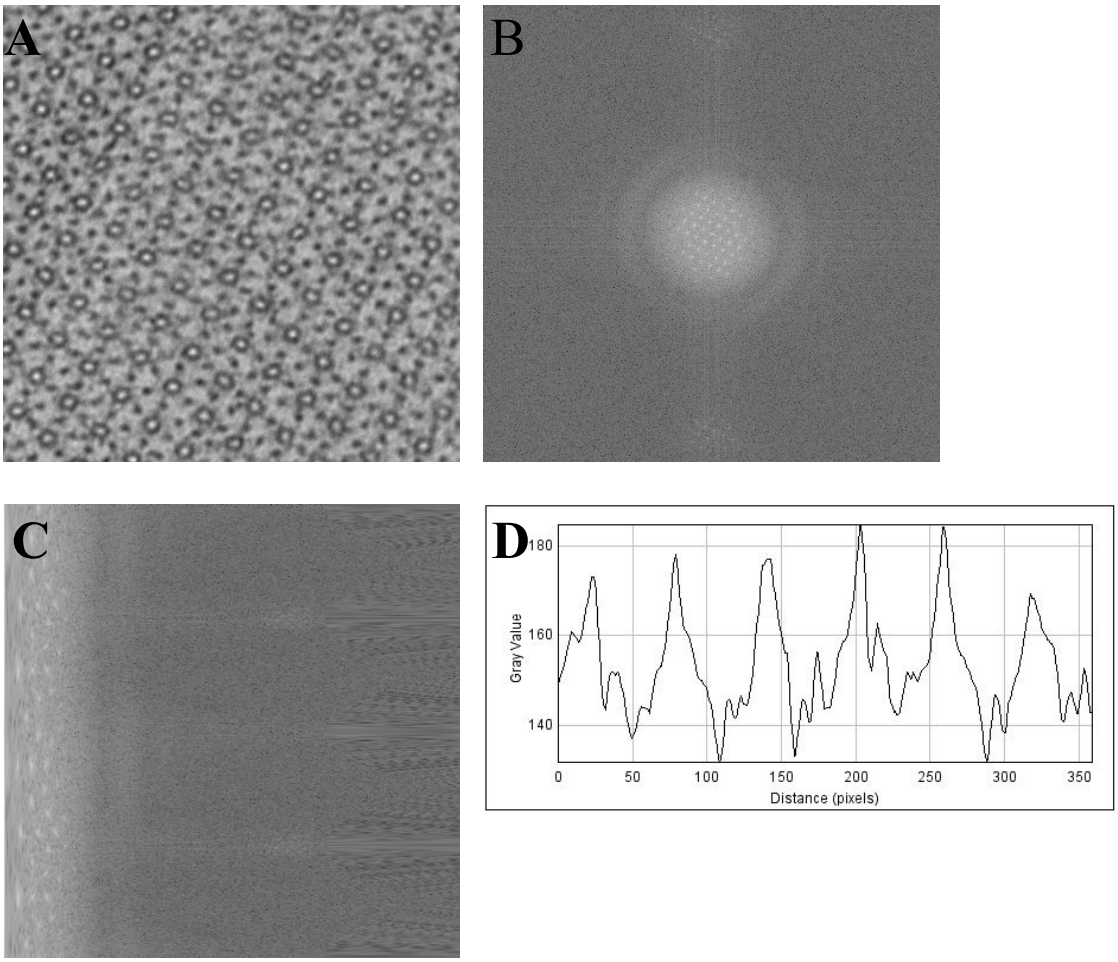

Figure 9: Electron microscopy cross section of *fln*$^{+}$ IFM myofibril. (A) 512 X 512 pixel area of individual myofibril. (B) FFT of image in (A), (C) Polar Transform of FFT, (D) Plot graph of Polar Transform.

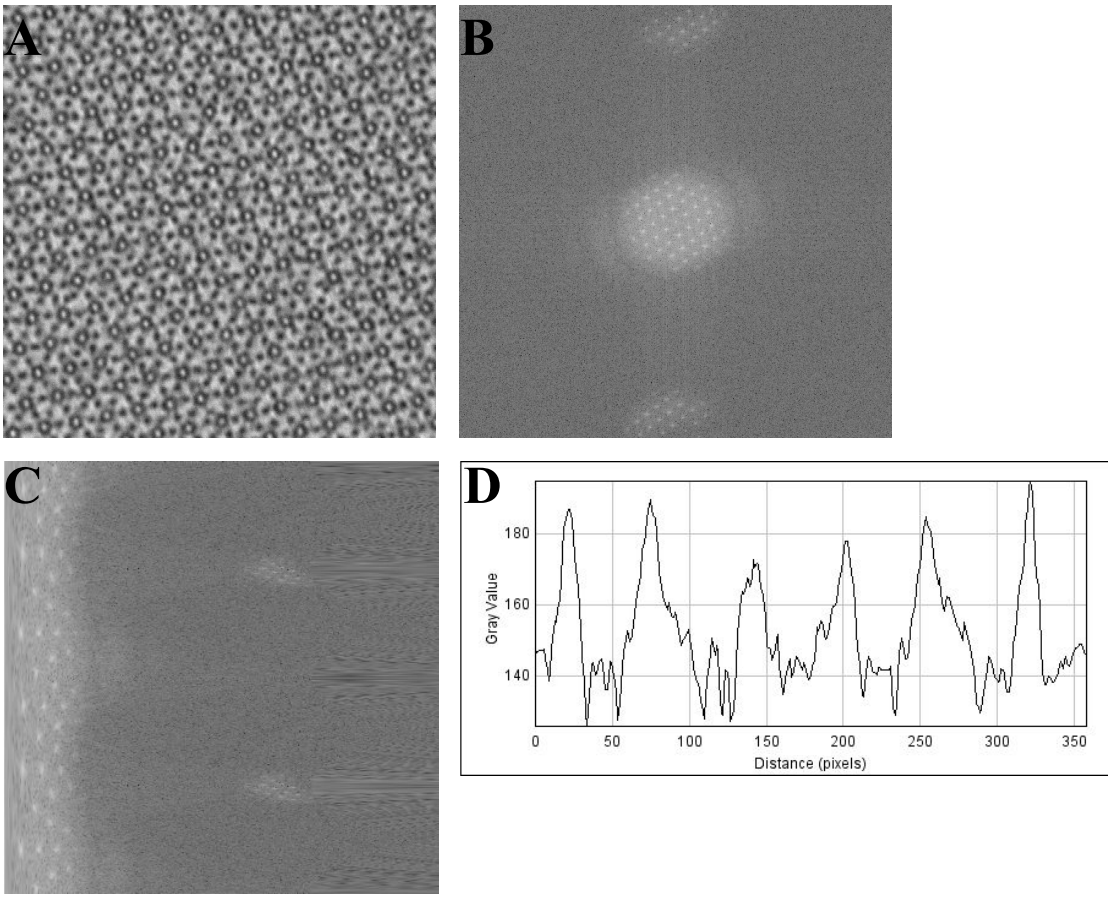

Figure 10: Electron microscopy cross section of *fln*^{virnch95} IFM myofibril. (A) 512 X 512 pixel area of individual myofibril. (B) FFT of image in (A), (C) Polar Transform of FFT, (D) Plot graph of Polar Transform.

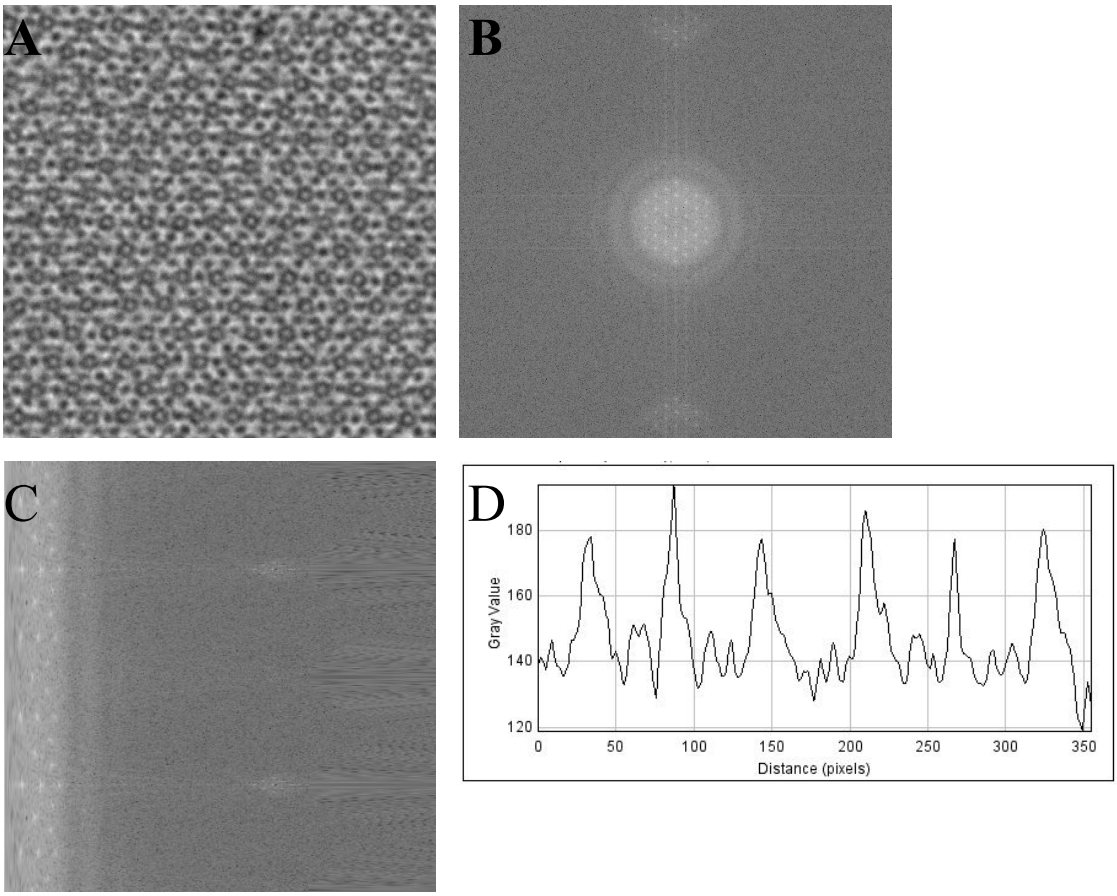

Figure 11: Electron microscopy cross section of *fln*^{virnch96} IFM myofibril. (A) 512 X 512 pixel area of individual myofibril. (B) FFT of image in (A), (C) Polar Transform of FFT, (D) Plot graph of Polar Transform.

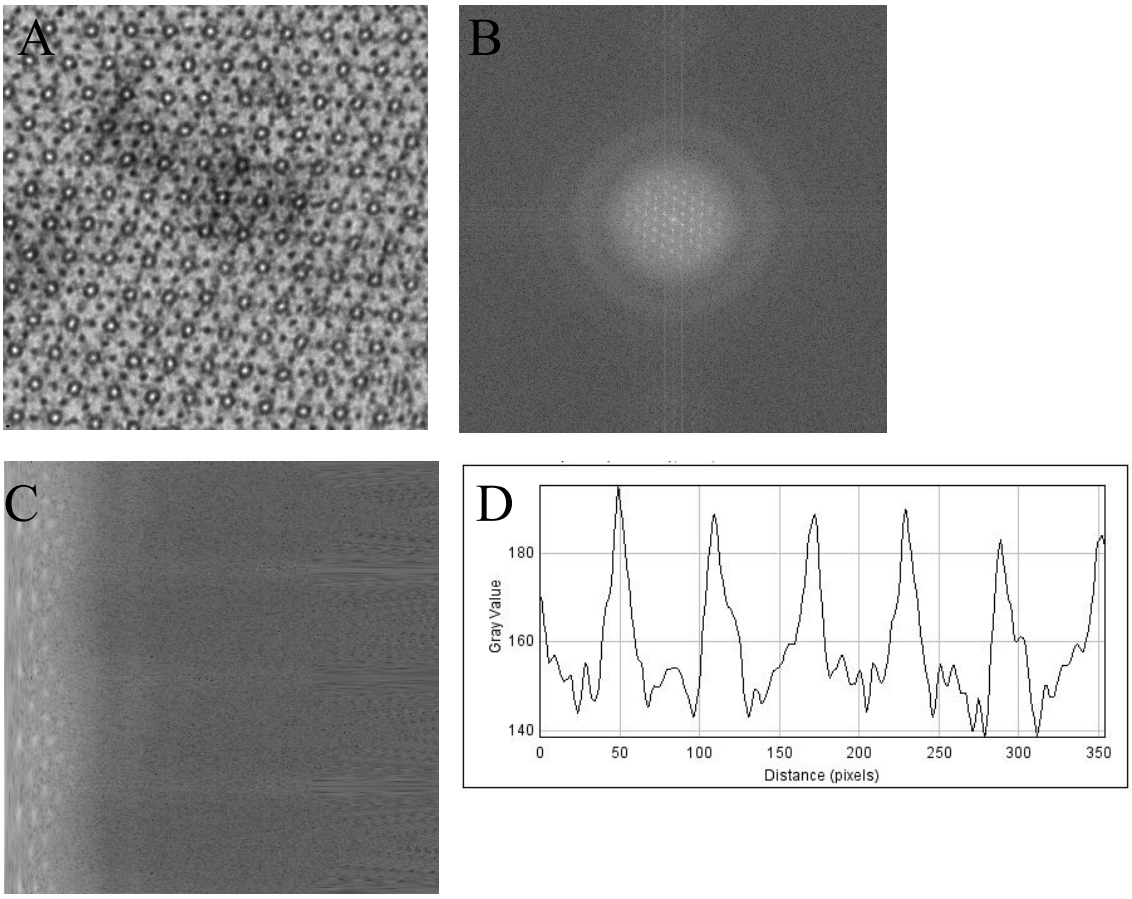

Figure 12: Electron microscopy cross section of *D.virilis* IFM myofibril. (A) 512 X 512 pixel area of individual myofibril. (B) FFT of image in (A), (C) Polar Transform of FFT, (D) Plot graph of Polar Transform.

Table 1: Myofibril analysis from electro micrographs.

Fly Line	$d_{1,0}$ (nm)	Inter-thick filament spacing (nm)	Resolution (nm)	1,0 Peak Intensity (1,0)	1,0 Half-width (pixels)
fln^{+}	40.013 ± 0.235	46.203 ± 0.271	10.940 ± 0.014	1.788 ± 0.007	13.203 ± 0.484
fln^{virnch95}	43.756 ± 0.449*	50.525 ± 0.519*	11.722 ± 0.079*	1.853 ± 0.010*	10.428 ± 0.193*
fln^{virnch96}	44.054 ± 0.387*	50.869 ± 0.446*	11.745 ± 0.101*	1.835 ± 0.011*	10.015 ± 0.215*
D.virilis	33.318 ± 0.717$^{*+\wedge}$	38.473 ± 0.828$^{*+\wedge}$	9.288 ± 0.141$^{*+\wedge}$	1.875 ± 0.010$^{*\wedge}$	14.044 ± 0.403$^{+\wedge}$

Asterisks (*) indicate significant difference; $p < 0.05$ compared to control *fln*$^{+}$. Plus signs (+) indicate significant difference; $p < 0.05$ compared to *fln*^{virnch95}. Carrot signs (^) indicate significant difference; $p < 0.05$ compared to *fln*^{virnch96}. For each sample n = 20

Both chimeric flightin lines *fln*^{virnch95} and *fln*^{virnch96} are significantly different from the control *fln*$^{+}$ line in all 5 parameters, *D.virilis* is significantly different from the control *fln*$^{+}$ line in all parameters except 1,0 Half- width. *D.virilis* is significantly different from *fln*^{virnch95} in all parameters except 1,0 Peak Intensity and significantly different from *fln*^{virnch96} in all 5 parameters. The highest resolution is seen in *D.virilis* and the lowest in the chimeric lines *fln*^{virnch95} and *fln*^{virnch96}. In addition myofilament lattice spacing is largest in the chimeric lines *fln*^{virnch95} and *fln*^{virnch96} and most compact in the *D.virilis* line, as seen by the values in $d_{1,0}$ and inter-thick filament spacing parameters.

To gain insight into the functional consequences of the differences in myofibril lattice parameters, mating competition assays were conducted as summarized in Table 2 in order to obtain the female preference and look for successful copulation.

Table 2: Combination of flies per competition assay

	Competition Assay # 1	Competition Assay # 2	Competition Assay # 3	Competition Assay # 4
Male 1	fln^{+}	*D. virilis*	fln^{+}	*D. virilis*
Male 2	$fln^{virnch95}$ or $fln^{virnch96}$	$fln^{virnch95}$ or $fln^{virnch96}$	$fln^{virnch95}$ or $fln^{virnch96}$	$fln^{virnch95}$ or $fln^{virnch96}$
Female	*D.melanogaster*	*D.virilis*	*D.virilis*	*D.melanogaster*

A total of 4 competition assays were each recorded for 30 minutes, but were not analyzed due to time restraints; 2 competition assays were recorded for #1, 1 competition assay was recorded for each of #2 and #3, and 0 competition assays were recorded for competition assay #4. Figures 13,14, and 15 represent a clip of individual competition assays videos. The following competition assay videos have been recorded, and are to be analyzed at a later date.

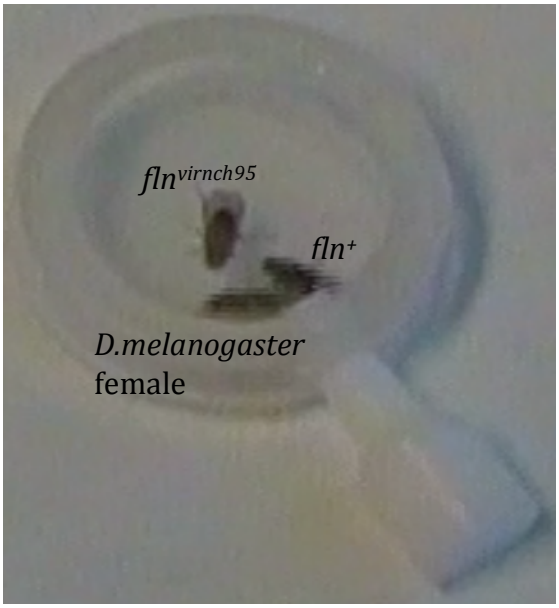

Figure 13: Competition assay #1

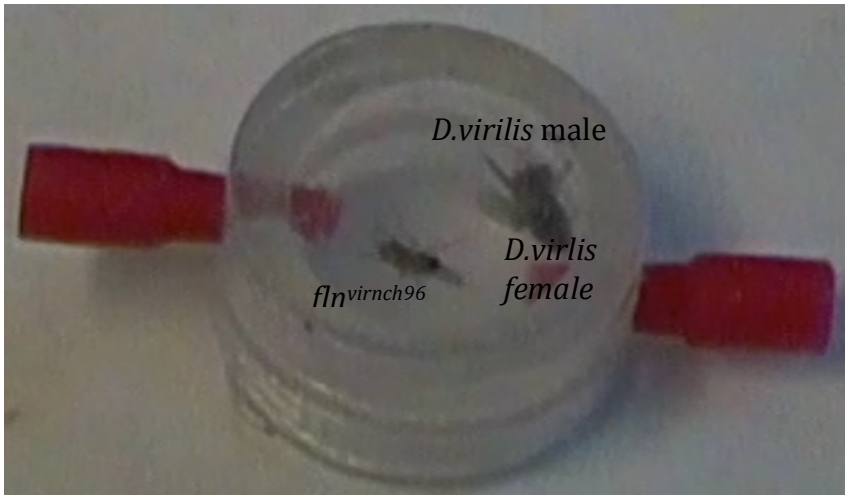

Figure 14: Competition assay #2

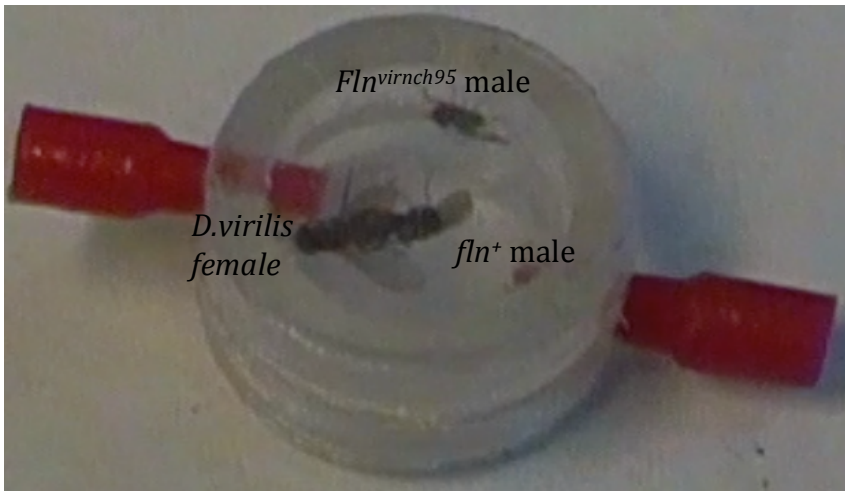

Figure 15: Competition assay #3

V. Discussion:

Skilled flying insects including *Drosophila* have been shown to have evolved a crystalline, highly regular thick and thin filament lattice organization in the asynchronous indirect flight muscles (IFM) responsible for powering flight. Various degrees of structural regularity suggest that the demand for skillfull flight has driven the lattice structure towards increased regularity (Iwamoto *et al* 2006). The purpose of this study is to investigate whether the sequence of amino acids in the flightin N-terminal region is under evolutionary pressures to optimize crystalline lattice structure.

Previous studies have shown that deletions of individual domains of flightin cause specific complications. Both the fln^{0} and the C-terminal truncation lines show abnormal and decreased myofilament lattice organization and other complications of muscles that results in the flies' inability to beat their wings, therefore abolishing flight and male courtship song production. These results render the C-terminal domain necessary for normal myofilament lattice organization, flight ability and male courtship song production (Tanner *et al* 2011).

The unique result of the 62 AA N-terminal truncation left the deletion line capable of flight and production of male courtship song, even though an abnormal myofilament lattice structure and decreased flight ability compared to fln^{+} was observed.

The flight test data in this study showed $fln^{virnch95}$ and $fln^{virnch96}$ fly as well or better than the fln^{+} control line. This indicates that the Chimeric flightin *virilis* gene is nontoxic, and that *D.melanogaster* can tolerate the *virilis* N-terminal sequence. The significant difference in flight ability between $fln^{virnch95}$ and $fln^{virnch96}$ females can be attributed to position effect i.e., transgene interference with certain genes during creation

of the chimeric lines. This significant difference is only seen in the flight tests, all other tests result in no significant difference between the two chimeric lines. The WBF of $fln^{virnch95}$ and $fln^{virnch96}$ had an intermediate value between fln^{+} and *D.virilis.* Electron microscopy revealed both chimeric lines $fln^{virnch95}$ and $fln^{virnch96}$ have an intermediate value in 3 out of the 5 parameters: $d_{1,0}$, Inter-thick filament spacing, and resolution with fln^{+} having the largest values, and *D.virilis* having the lowest and more compact structure. A larger $d_{1,0}$ indicates a greater distance between the consecutive thick filament planes as seen in Figure 3, a larger inter-thick filament spacing value indicates a greater distance between adjacent thick filaments, and a lower resolution value means two adjacent points are better distinguished. Lower peak intensities and broader half-width indicate more variability in the spacing between lattice planes across the cross-section of the myofibril, reflecting a more heterogeneous lattice. The increase in heterogeneity of the lattice structure seen in the chimeric line can be attributed to various other muscle protein-protein interactions. In addition, it might be a result of the difference in level of flightin expression seen between the control and chimeric lines.

The data shows that the N-terminal domain contributes to the characteristics of WBF of each species, and has an important role in defining myofilament lattice properties. Figure 4 shows the distinct difference in amino acid sequence, with *D.virilis* containing a greater abundance of acidic amino acids. A possible explanation can therefore incorporate the use of electrostatic repulsion. Due to the acidic residues of the N-terminal region being greater on the *D.virilis* (pI= 3.76 using ExPASy), compared to *D.melanogaster* (pI= 3.82 using ExPASy) (Artimo P *et al* 2012) the N-terminal swap resulted in the chimeric line having a greater amount of acidic residues, which led to a

lower pI and thereby a greater negative charge. Recalling that flightin binds to the myosin rod which is negatively charged, it is possible that added negative charge of the N-terminal due to the swap, results in electrostatic repulsion with the myosin rod generating greater $d_{1,0}$ and inter-thick filament distances. If the charge of the N-terminal domain is solely responsible for dictating inter-thick filament distances, one would predict $d_{1,0}$ spacing to be greatest in *D. virilis*. One reason why this is not seen in *D.virilis* can be attributed perhaps to protein interaction unique to or different within the *D.virilis* IFM that causes the extra negative charges to be neutralized. Further studies should investigate the effects of adding a highly acidic, basic, and neutral amino acid N-terminal sequence to note if the change in crystalline lattice structure supports the electrostatic repulsion or attraction theory.

IFM is of interest in that it underlies two distinct behaviors; flight and mating song. Therefore the crystallinity needs to be able to optimize both characteristics, and is predicted to be competing under dual-selection pressures; natural selection and sexual selection to optimize flight and the courtship mating song, respectively. In order to understand which selection pressure has the greater influence, future research should investigate the mating competition assays to see if female preference favors a specific flightin gene over another. In addition mating song analysis should be completed to see if the N-terminal region has any influence on specific song parameters and if these altered parameters in the sine and pulse song increase the likelihood of female preference and ultimately successful copulation. With the compilation of the electrostatic repulsion or attraction data, male courtship song analysis, and mating competition assays we can

potentially be able to link amino acid sequences in the N-terminal region to which parameter in the IFM they influence; flight or mating courtship song.

VI. References:

Artimo P, Jonnalagedda M, Arnold K, Baratin D, Csardi G, de Castro E, Duvaud S, Flegel V, Fortier A, Gasteiger E, Grosdidier A, Hernandez C, Ioannidis V, Kuznetsov D, Liechti R, Moretti S, Mostaguir K, Redaschi N, Rossier G, Xenarios I, and Stockinger H. ExPASy: SIB bioinformatics resource portal, *Nucleic Acids Res*, (2012) 40(W1):W597-W603.

Ayer G, Vigoreaux J (2003) Flightin is a myosin rod binding protein. Cell Biochem Biophys. 38(1):41-54.

Barton B, Ayer G, Heymann N, Maughan D, Lehmann F, Vigoreaux J (2005) Flight muscle properties and aerodynamic performance of Drosophila expressing a flightin transgene. J Exp Biol, 208(Pt 3):549-560.

Chakravorty S, PhD (2013) Role of the *Drosophila melanogaster* indirect flight muscles in flight and male courtship song: studies on flightin and myosin light chain-2. PhD Thesis. University of Vermont.

Contompasis J, Nyland L, Maughan D, Vigoreaux J (2010) Flightin is necessary for length determination, structural integrity, and large bending stiffness of insect flight muscle thick filaments. J Mol Biol. 395(2):340-8.

Dickinson M, Fry S, Sayaman R (2005). The aerodynamics of hovering flight in Drosophila. *Journal of Experimental Biology*, *208*(12), 2303-2318.

Dudley R, (2000) The biomechanics of insect flight. Princeton: Princeton University Press.

Iwamoto H, Inoue K, Yagi N (2006) Evolution of long-range myofibrillar crystallinity in insect flight muscle as examined by X-ray cryomicrodiffraction. Proc Biol Sci 273(1587): p. 677-85.

Reedy M, Bullard B, Vigoreaux J (2000) Flightin is essential for thick filament assembly and sarcomere stability in Drosophila flight muscles. J Cell Biol. 151(7):1483-500.

Snodgrass R (1935) Principles of Insect Morphology. New York: McGraw-Hill Book Co.

Tanner B, Daniel T, Regnier M (2007) Sarcomere lattice geometry influences cooperative myosin binding in muscle. PLoS Comput Biol, 3(7): p. e115.

Tanner C, Miller M, Miller B, Lekkas P, Irving T, Maughan D, Vigoreaux J (2011) COOH-terminal truncation of flightin decreases myofilament lattice organization, cross-bridge binding, and power output in Drosophila indirect flight

muscle. Am J Physiol Cell Physiol. 301(2):C383-91.

Vigoreaux J, Saide J, Valgeirsdottir K, Pardue M (1993) Flightin, a novel myofibrillar protein of Drosophila stretch-activated muscles. J Cell Biol 121:587-598.